Absolute soot volume fraction measurement by laser induced incandescence calibration in sooting turbulent diffusion flame

H Q Do, L D Ngo, Y Carpentier, Xavier Mercier, Eric Therssen

Absolute soot volume fraction measurement by laser induced incandescence calibration in sooting turbulent diffusion flame

H.Q Do[1], L.D Ngo[1,2], Y Carpentier[2], X Mercier[1],E Therssen [*1],

[1]Univ. Lille, CNRS, UMR 8522 – PC2A – Physicochimie des Processus de Combustion et de l'Atmosphère, 59000 Lille, France

[2]Univ. Lille, CNRS, UMR 8523 – PhLAM – Laboratoire de Physique des Lasers Atomes et Molécules, 59000 Lille, France

Abstract

This paper mainly describes the laser based method we developed for quantitative measurements of soot volume fraction applied in two turbulent flames of diesel and E85 (gasoline/ethanol mixture) stabilized on a home-made jet burner working with liquid fuels. The two flames have been studied by keeping constant the lower heating value (LHV) at atmospheric pressure. The diesel flame was a normal sooting flame which generates soot particles from inception to mature stage. The second flame was an E85 flame producing very small amounts of soot particles that do not undergo or very limited surface growth along the height above the burner. We propose here a new auto-calibrated laser induced incandescence method for the detection system specifically develop to directly determine the soot volume fraction (f_v) in sooting turbulent diffusion flame, relying on the LII spectrum measurement. The experiments were carried out by using a laser at 532 nm and required the temperature determination along the vertical center line of the flame necessary for the determination of the soot absorption function $E_m(\lambda)$. This parameter allows to decrease the uncertainty for the soot volume fraction (f_v) value. The maximum soot volume fraction in the diesel flame around 951 ppb and 13 ppb in the flame E85 were determined this way, highlighting the very weak soot formation with the studied biofuel.

Keywords: Soot volume fraction, laser induce incandescence, diesel, bio-fuel, sooting turbulent diffusion flame

Introduction

The formation and emission of soot particles from fuel combustion have a harmful effect on the climate, environment and human health [1]. Soot volume fraction (f_v) measurement is a critical need to validate kinetic soot model in different combustion systems and for different fuels [2, 3]. A large panel of *in situ* and *ex situ* techniques have been used to quantify soot particles in flames. In that context, the scanning mobility particle sizing (SMPS) appears as a method of choice for the measurement of size distribution and number of soot particles and therefore soot volume fraction [4]. However, the SMPS is an intrusive method, hardly usable for turbulent flames which moreover requires the dilution of the species along a sampling line that can lead to alteration of the sampled particles (notably of the smallest particles by condensation or coagulation). By comparison, optical method as extinction or LII enable soot volume fraction measurements in flames without intrusive sampling probes or sensors. Moreover, laser diagnostic techniques possess highly spatial and temporal resolution better adapted to turbulent flame studies. LII is a conventional technique which has been widely used to measure soot particles in flames [5]. Nevertheless, the absolute value of soot volume fraction cannot be determined only through the LII technique which needs other measurement approaches to calibrate the LII signals, as by the complementary use of the laser extinction method [6,7]. To simplify the f_v measurement by LII, we propose here a new auto-calibrated laser based method we developed for quantitative measurements of soot volume in the context of turbulent flames, based on the recording of the LII spectrum in the near IR region and the calibration of the detection system by using a black body radiation source of measured luminescence. As an application of the method we first determined the f_v in a turbulent diesel flame which generates soot particles from inception to mature soot. Then we applied the method in very slight sooting flame of commercial biofuel (E85) highlighting both the sensitivity of the technique and the very amount of soot produced in this last flame.

Experimental set-up

Burner and flame conditions

The spray jet flames in this study are generated in a home-made burner at atmospheric pressure as presented in Fig.1. The burner is equipped with a direct liquid injection high efficient nebulizer (DIHEN-170-AA). This nebulizer allows us to transform the liquid fuel into very small droplets (7 – 18 µm) which are able to vaporize quickly. This type of injector required a gas flow supply with high speed as the driving force for liquid atomization. In our work, the nitrogen is used as nebulization gas. The liquid fuel was introduced in the nebulizer capillary and was regulated by a liquid mass flow controller from Bronkhorst, model M13V14I with mass flow accuracy of ± 0.2%. The oxidation air flows enter the burner from two symmetrized sides and are homogenized with the help of a honeycomb. The gas flow rates of N_2 and air were measured by using regulated mass flow controllers (Bronkhorst) with mass

* Corresponding author: eric.therssen@univ-lille.fr

flow accuracy of ± 0.5%. The burner was mounted on a vertical translation stage allowing to modify the burner position on the vertical axis with 1µm precision.

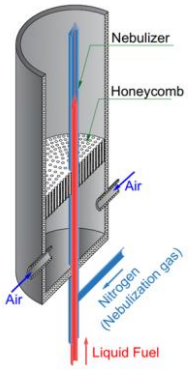

Fig.1. Sketch of the burner generating the jet spray flames

The conditions of the two studied flames are summarized in table 1. The LHV of diesel around 43 $MJ.kg^{-1}$ [8] is higher than that of gasoline E85 around 29.1 $MJ.kg^{-1}$. The LHV of E85 was calculated from the LHV of ethanol around 26.8 $MJ.kg^{-1}$ [9] and gasoline SP95 around 43.2 $MJ.kg^{-1}$ [10] for the mixture (15% SP95 / 85% ethanol) in volume. Thus, the mass flow rate of E85 flame was adjusted to produce the same LHV than the diesel flame.

Flame	Fuel ($g.h^{-1}$)	Air ($NL.min^{-1}$)	Nebulization N_2 ($NL.min^{-1}$)	LVH ($MJ.h^{-1}$)
Diesel	98.2	19.6	0.25	$4.2.10^{-3}$
E85	145.4	19.6	0.25	$4.2.10^{-3}$

Table 1: Flame conditions

Temperature measurement

The vertical center line temperature profiles of the two flames were measured with a type S thermocouple (TC S.A., Pt-Pt/10%Rh) having 0.35 mm wire diameter and 1.01 mm bead diameter measured with a 5 µm sensitivity micrometer. The thermocouple was inserted radially into the centerline of the turbulent flames at different HABs by using a motorized remote-controlled system. The soot particle movement in turbulent flames is very fast, allowing to minimize the soot deposit on the thermocouple. The thermocouple was cleaned by using a lean flame after each three measurements in the sooting zone. The thermocouple temperature measurements were corrected from the radiation losses according to procedure described in Elias et *al* [11]. Temperature uncertainties were estimated this way to be ± 100 K.

LII experiment

The LII experiments have been carried out by using a 532 nm laser excitation wavelength after frequency doubling of the fundamental 1064 nm wavelength generated by a Nd: YAG Quantel. The 6 ns laser pulse was cadenced at 10 Hz. The energy of the laser beam was adjusted with an attenuator module. Two prisms were used to direct the laser beam through a circular pinhole with diameter of 850 µm in order to obtain a laser beam with a top hat profile. The laser beam at the exit of the pinhole was sent at the center of the burner using a focus lens with 200 mm focal length. This lens was placed at two times the distance of its focal length between the pinhole and the burner in order to avoid the diffraction patterns of the laser spot and to obtain a top-hat profile into the diameter of the flame. The laser beam energy was measured by using a laser pyroelectric energy sensor located just after the burner (no-extinction of the laser was measurable due to low volume fraction of soot and low flame diameter).

The incandescence emission from the flame was collected through the entrance slit of a spectrometer using two achromatic lenses (f_1=400mm and f_2=200mm) setting a magnification factor of 0.5. A Notch filter 532 ± 9.8 nm was located just before the spectrometer to remove part of the 532 nm laser scattering. The emission signal through the notch filter was collected with an Acton SP300i spectrometer through a 1 mm wide opened slit. A diffraction grating 150 groves/mm, blazed at 800 nm (high transmission in near IR) was used. The center wavelength of the diffraction grating was set at 750 nm allowing to collect the emission spectral range from 609.1 nm to 889.8 nm. The spectrometer has two outputs provided to collect the signal either by a photomultiplier tube Philips XP2020Q (PMT) or by a Roper PIMAX 4 ICCD camera.

Temporal LII signals measured by PMT were triggered by a photodiode detector and typically averaged over 2000 laser shots. 1D spectral measurements were recorded with a temporal detection gate (gate width of the camera) set to 50 ns and centered on the peak of the LII pulse. 1D spectral images were recorded in order to obtain the emission spectra for the chosen wavelength domain or to obtain the flame emission profile. 1D spectral images were obtained by averaging 500 images and systematically corrected from the corresponding average background emission of the flame.

Calibrated lamp

In this work, we propose a new direct method to calibrate the soot volume fraction from the LII signal measured by the ICDD camera. To do so, we used an integration sphere from SphereOptics CSTM-LR-6-M. This sphere consists of a lamp located inside of a cavity, which is covered by white Lambertian substrate (BaSO4). It emitted a black body type radiation in the range of 360 nm to 1000 nm with an adjustable temperature between 2000 and 3300 K by adjusting the voltage of the external power supply module. An optical fiber connected with the sphere directs the light to a calibrated spectrograph, which provides luminance L° spectra as reference. This optical configuration is represented in the Fig. 2.

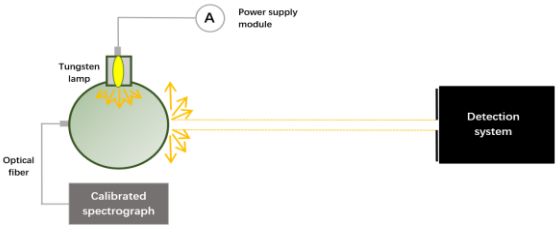

Fig.2. Schematic of the optical set up for the calibration with sphere

The parameters of the detection system (position of the collimator, gain of the camera) are the same as for LII measurements.

The power *P* emitted by the orifice of the sphere per steradian (meaning the product of the luminance L° given by the calibrated spectrometer of the sphere by the sphere orifice surface $S_{sphere\ orifice}$ and by the wavelength bandwidth Δλ) for different power supply of the tungsten lamp (meaning different color temperatures of black body photons) is according to:

$$P = L^{\circ} . S_{sphere\ orifice} . \Delta\lambda \qquad eq\ 1$$

For the detection system, the response (in count) of one pixel of the CDD could expressed as:

$$S_{CCD} = L^{\circ} \cdot \Delta\lambda \cdot S_{1\ pixel} \Omega\, \beta \qquad eq.2$$

where $S_{1\ pixel}$ (m^2) is the surface area of the collected image in the space corresponding to one pixel in the ICCD camera, Ω (sr) is the collection solid angle from a photon emitted from the sphere to the first collection lens, β (count.W^{-1}) is the transmission coefficient, which depends on the set up of the experiment and the detected wavelength range.

All calculations in this study have been realized for 1 pixel corresponding to λ = 800.05 nm. The luminance of the sphere L° at 15V and λ = 800.05 nm is $1.2325.10^9$ ($W.m^{-2}.m^{-1}.sr^{-1}$). The Δλ which depends on the grating of the spectrograph and the camera is $2.74.10^{-10}$ (m). $S_{1\ pixel}$ can be obtained with $S_{1\ pixel} = 2 \times h_{slit} \times 2 \times l_{pixel}$ due to the presence of the achromatic lenses system. h_{slit} which is the height of the slit of the spectrograph is $1.19.10^{-3}$ (m). l_{pixel}, the size of 1 pixel is $1.3.10^{-5}$ (m). Thus, S_{1pixel} = $6.19.10^{-8}$ (m^2) and S_{CCD} measured by the camera at 15 V after correction by the transfer function is 1013.2 (count). From *eq.2*, we obtain a value of $\Omega\beta$ = $4.8472.10^{10}$ (count.sr.W^{-1}).

Results

Temperature profile

Fig. 3 shows the experimental temperature profiles measured in the center line of the diesel et E85 flames. The maximum temperatures of two flames are very similar. However, the temperature profile of E85 flame shifts 100 mm higher by comparing to that of the diesel flame. This shift could be explained by the difference of the mass flow rate of the fuels (145.4 $g.h^{-1}$ for the E85 and 98.2 $g.h^{-1}$ for diesel flame).

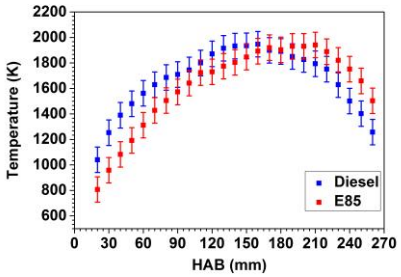

Fig.3. Temperature profiles measured in the center line of diesel et E85 flames

LII results

Laser fluence determination

The evolution of the LII signal as a function of the laser fluence along the center line of the flame has been studied for the two flames and reported in Fig.4 (left column). In the diesel flame, the fluence curves shape clearly varies with HAB. This evolution is characteristic of the evolution of the optical properties ($E_m(\lambda)$ notably) of the generated soot particles. At 50mm HAB, the fluence curve is quasi-linear with energy as generally observed for nascent soot particles in laminar flames [5]. At 70 mm HAB, the fluence curve starts to bend and to finally leads above this HAB to the typical S shape of fluence curves characteristic of mature soot [5]. From HAB equal to 110 and 200 mm, the fluence curves peaks around 100 $mJ.cm^{-2}$ before decreasing when laser fluence increases due to soot sublimation above this laser fluence.

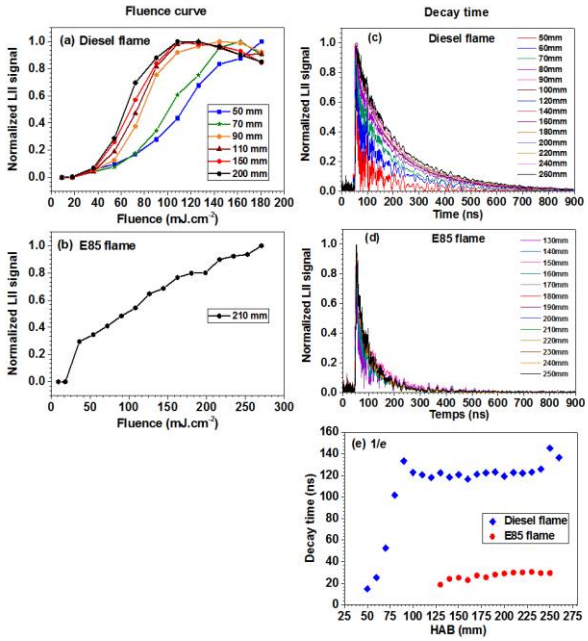

Fig.4. Left column: Normalized fluence curves obtained in diesel and E85 flame. Right column: LII temporal signal measured at different HAB in two flames: (a) diesel flame, (b) E85 flame. For clarity, the peak of LII signals have been normalized to 1 (c, d). (e) LII decay-time measured at 1/e of the LII signal as a function of HABs

The corresponding temporal decay curve of the LII is reported in the right column of Fig.4 (Fig.4c and d) as well as the measured decay-times at 1/*e* (Fig.4e) of the LII peak signals. The relationship between the LII temporal decay and soot particle size is complex [12] and requires the use of LII modeling to interpret the LII signal in terms of primary particle diameter. However, the evolution of the temporal LII decay time is correlated to the diameter of soot particle [12]. The longer the decay time is larger the soot particle size. In the diesel flame, the decay-times increase from 50 mm to 90mm and remain nearly constant at higher HABs. This evolution indicates that the nascent soot particles which are formed around 50 mm HAB, undergo soot growth process with HABs until 90 mm HAB.

Regarding the E85 flame, we could only determine the fluence curve at 210 nm because of the very weak LII signal, especially for the lower HAB. The quasi-linear shape of the obtained fluence curve seems to characterize the formation of nascent soot particles (with low $E_m(\lambda)$ value) undergoing only limited or no surface growth along the flame height. This statement is corroborated by the absence of increase of the LII decay-times reported also in Fig.4d indicative of nascent soot particles. As can be seen, the corresponding decay-times measured at 1/*e* of the LII peak signals remain constant for all HABs in the E85 flame and very close the value determined at 50 mm and 60 mm in the diesel flame.

LII imaging of the flame

Regarding the fluence curve, we defined a laser fluence around 54 mJ.cm^{-2} for the LII measurement in the diesel flame with the ICCD camera. This value allows indeed LII measurements without sublimation issues and an adequate signal to noise ratio. In the E85 flame where no sublimation issue can be established until 250 mJ/cm^2, we had to increase the laser fluence to 108 mJ.cm^{-2} in order to get a sufficient signal to noise ratio for the LII measurement.

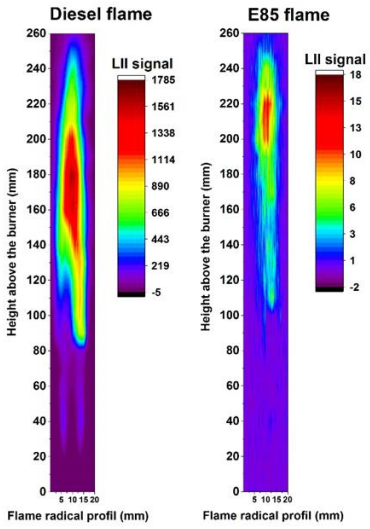

Fig.5. 2D plots of LII signal detected at 800 nm

The temporal gate width of the camera was also chosen regarding these data. We hence defined a starting gate at the peak of LII signal and a with a gate width of 50 ns, allowing to minimize the variation of temperature between t = 0 ns and t = 50 ns during the measurement of the heated soot particles. In our experimental condition, we have estimated this variation around 8.5 %.

Fig.5 shows the rebuilt LII images obtained from series of 1D spectral measurements centered at 800 nm. We note that the maximum LII signal along the center line of the flames appears at 180 mm of HAB in the diesel flame. The corresponding LII signal intensity is 100 times higher than that the maximum LII signal determined 210mm HAB in the E85 flame.

Absolute soot volume fraction determination

The absolute soot volume fraction has been experimentally determined along the center line of the two flames according to the new auto-calibrated method presented below and described step by step.

Determination of the temperature of the heated soot

The average temperature T_p of the soot particles heated by the laser can be derived from the LII spectrum as below:

$$\ln\left(\frac{S_{LII}(t_0,\lambda)\lambda^6}{E_m(\lambda)}\right) = -\frac{hc}{k_b T_p \lambda} + \ln(48\pi hc^2 f_v) \qquad eq.3$$

where $S_{LII}(t_0,\lambda)$ is the incandescence signal intensity, $E_m(\lambda)$ the absorption function of the particle, T_p the average temperature of soot particles and f_v the soot volume fraction.

To determine T_p, we first need to record an emission LII spectrum in a spectral range (750-850 mm) within $E_m(\lambda)$ can be assumed as constant [13]. In that case, the relation $ln(S_{LII}(t_0,\lambda)\lambda^6 \sim -hc/(k_b,T_p)$ can be established. Fig. 6 presents some examples of T_p determination from LII spectra in the diesel et E85 flames.

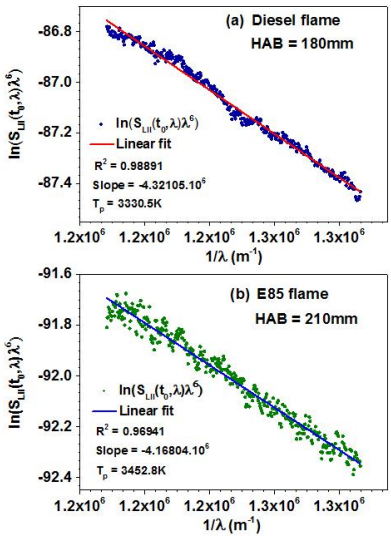

Fig.6. Determination of T_p from two LII spectra: (a) Diesel 180mm, (b) E85 210mm

The LII signal were measured in the flame center and corrected from the transfer function and flame emission for the calculation process. Good linear fits are obtained for the diesel and E85 flame, allowing an accurate the heated temperature of the particles for all HAB.

LII signal intensity from soot particles

Soot particles are known to behave as grey body emitter characterized by the following expression:

$$E_{bb}(T_p,\lambda) = \int_{\lambda_1}^{\lambda_2} \varepsilon(T,\lambda)\frac{2\pi hc^2}{\lambda^5}\frac{1}{exp\left(\frac{hc}{\lambda k_B T_p}\right)-1} d\lambda\, dS \qquad eq.4$$

where E_{bb} is the emittance (W) of an elementary surface dS (m^{-2}) emitted over 2π steradian (in "half the space") and defined over a spectral range $d\lambda$. $\varepsilon(T,\lambda)$ is the emissity (without dimension).

The absorbing ability $\alpha(\lambda,T_p)$ of a body represents the ratio of the radiation flux absorbed by the body to the radiation flux incident on the body. According to Kirchhoff's law, the emissivity is equal to the absorption coefficient for the same couple of λ and T_p values. The emissivity is given in the Rayleigh approximation by, where $\pi d_p << \lambda$

$$\alpha(\lambda,T_p) = \frac{4\pi\, d_p E_m(\lambda)}{\lambda} \qquad eq.5$$

The Kirchhoff's law establishes the relationship between the abilities of emitted and absorbed electromagnetic energy by any physical body. It can therefore be approximated that the heated soot particles are in thermodynamic equilibrium with the encountered radiation. So the absorption coefficient $\alpha(\lambda,T_p)$ and the emission coefficient (or emissivity) $\varepsilon(\lambda,T_p)$ are equal for the same couple of T_p, λ.

Thus, according to *eq.5*, the emissivity could be taken into account to define the *eq.6* for a defined volume V, which contains N_p (m^{-3}) soot particles (spherical particles in the Rayleigh approximation, here with the same diameter and a surface of πd_p^2). The following equation gives the LII signal emitted by N_p soot particles:

$$S_{LII}(T_p,\lambda) = \int_{\lambda_1}^{\lambda_2} N_p.\frac{4\pi\, d_p E_m(\lambda)}{\lambda}.\ \pi d_p^2.\frac{2\pi hc^2}{\lambda^5}\frac{1}{exp\left(\frac{hc}{\lambda k_B T_p}\right)-1} d\lambda \qquad eq.6$$

Considering the soot volume fraction f_v defined as $f_v = N_p\frac{\pi d^3}{6}$, the LII signal $S_{LII}(T_p,\lambda)$ in W.m^{-3} emitted at 4π steradian can finally be expressed as:

$$S_{LII}(T_p,\lambda) = \int_{\lambda_1}^{\lambda_2} \frac{48\pi^2 hc^2 E_m(\lambda)}{\lambda^6}\frac{1}{exp\left(\frac{hc}{\lambda k_B T_p}\right)-1} d\lambda f_v \qquad eq.7$$

Eq.7 represents the general equation of the LII signal characterizing the thermal radiation emitted by N_p spherical soot particles at the temperature T_p according to their optical properties $E_m(\lambda)$ in the investigated wavelength domain. As, the emission spectral range $\Delta\lambda$, centered on λ, is very narrow, the expression of the total LII signal emitted at 4π steradian in W.m^{-3} could be expressed as:

$$S_{LII}(T,\lambda) = \frac{48\pi^2 hc^2 E_m(\lambda)}{\lambda^6}.\frac{1}{exp\left(\frac{hc}{\lambda k_B T_p}\right)-1}.\Delta\lambda\,.\,f_v \qquad eq.8$$

The LII signal from soot particles were measured with the detection system characterized by the collection solid angle Ω and the transmission coefficient β. Thus, S_{LII} detected could be expressed as:

$$S_{LII,detected}\ (T_p,\lambda) = \frac{12\pi\, hc^2 E_m(\lambda)}{\lambda^6}.\frac{1}{exp\left(\frac{hc}{\lambda k_B T_p}\right)-1}.V_m\,.\,\Omega\,.\,\beta\,.\,\Delta\lambda\,.\,f_v \qquad eq.9$$

where V_m is measured volume with $V_m = 2\times l_{pixel}\times \frac{\pi\phi_{laser}^2}{4}\,.\,h_{slit}$. The diameter ϕ_{laser} of the 532nm excitation laser beam is 850µm. Thus, V_m = 1.475.10^{-11} m^3.

From *eq.9*, it appears that to determine the soot volume fraction, the $E_m(\lambda)$ values and corresponding temperatures of soot particles are necessary. In the low laser fluence regime, the $E_m(\lambda)$ absorption function can be expressed by:

$$E_m(\lambda) = \frac{(T_p-T_g).\lambda_{laser}.\rho_s.c_s}{6\pi.F} \qquad eq.10$$

where T_g is the temperature of flame, λ_{laser} is the laser wavelength, F the laser fluence, ρ_c the density of soot particles and c_s is the specific heat of soot particles. The density of soot ρ_c in the diesel flame was extrapolated from 1.3 g.cm^{-3} for nascent soot to 1.8g.cm^{-3} for mature soot [14]. The value of ρ_c in the E85 flame was considered constant and equal to 1.3g.cm^{-3} for all HABs. The value of specific heat of soot particles is taken at 2.3 J.g^{-1}.K^{-1} [14].

Fig.7 (a) presents the evolution of the average temperature of soot particles after laser pulse measured in the center line of two studied flames. The temperature of the soot particles in the flame E85 was slightly higher than that in the diesel flame because the laser fluence used for E85 flame was higher than that used for diesel flame. In the diesel flame, the resolution of the LII spectra from 50 mm HAB enable to determine the average temperature of soot particle while T_p could only be identified from 160mm to 240 mm HAB in the E85 flame. Fig.7 (b) shows the evolution of $E_m(\lambda)$ along the center line of the two studied flames. In the E85 flame, $E_m(\lambda)$ is nearly constant around 0.14 with the flame heights, characteristic of nascent soot particles In the diesel flame, the value of $E_m(\lambda)$ at the beginning of the soot formation is 0.226 which is higher than the value of the E85 flame. This difference might be explained by the turbulence of the diesel flame. The images recorded by camera might be mixture of signal coming from nascent particles formed in the central axis and more mature

ones surrounding the flame. Above 120mm HAB, $E_m(\lambda)$ increases with HABs due to the evolution of optical properties of the soot particles with their maturation.

The soot volume fraction profiles determined along the center line of two flames of diesel and gasoline E85 is finally presented in Fig.8. The experimental results show that the maximum soot volume fraction in the diesel flame is 951 ppb while it is only 13ppb in the flame E85. The method proposed in this study allows to measure the soot volume fraction in very slightly sooting flame. These results highlight that this kind of fuel is a promising bio-fuel for internal combustion engine in regard to the soot formation issues.

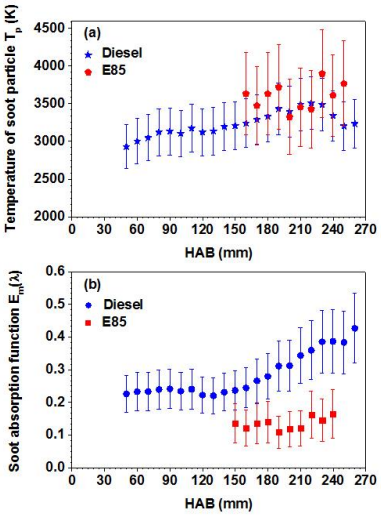

Fig.7. Evolution of temperature of soot particle (a) and $E_m(\lambda)$ (b) with HAB in two flames of diesel and E85. Laser fluence = 54 mJ.cm^{-2} for diesel flame and laser fluence = 108 mJ.cm^{-2} for E85 flame.

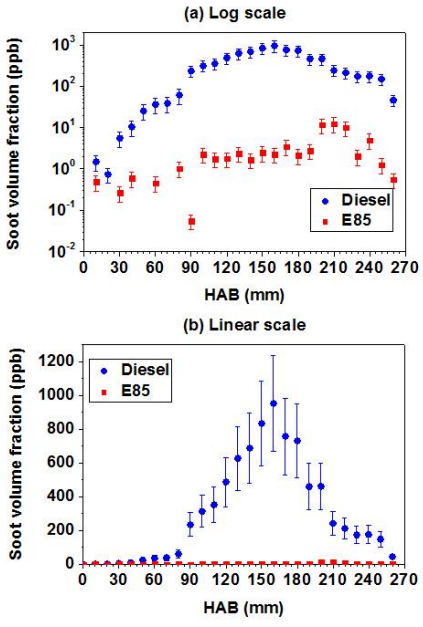

Fig.8. Soot volume fraction profile measured in the center line of diesel flame (blue) and of E85 gasoline flame (red).

4.Conclusion

This work describes a new auto-calibrated method of the detection system allowing a direct determination of the soot volume fraction by LII in flames. We demonstrated here that this method is well adapted for turbulent flame studies and highlight a large dynamic scale in terms of measurable soot volume fraction. This method provides here valuable information about the propensity of diesel and E85 biofuel to generate soot particles. With a produced soot volume fraction rather than 100 times lower than the diesel flame, the E85 appears a promising biofuel.

References

[1] J. Hansen, L. Nazarenko, Soot climate forcing via snow and ice albedos, Proc. Natl. Acad. Sci. 101 (2004) 423–428.

[2] H. Koo, M. Hassanaly, V. Raman, M.E. Mueller, K. Peter Geigle, Large-Eddy Simulation of Soot Formation in a Model Gas Turbine Combustor, Journal of Engineering for Gas Turbines and Power. 139 (2016).

[3] C. Betrancourt, D. Aubagnac-Karkar, X. Mercier, A. El-Bakali, P. Desgroux, Experimental and numerical investigation of the transition from non sooting to sooting premixed n-butane flames, encompassing the nucleation flame conditions, Combustion and Flame. 243 (2022) 112172.

[4] J. Camacho, C. Liu, C. Gu, H. Lin, Z. Huang, Q. Tang, X. You, C. Saggese, Y. Li, H. Jung, L. Deng, I. Wlokas, H. Wang, Mobility size and mass of nascent soot particles in a benchmark premixed ethylene flame, Combustion and Flame. 162 (2015) 3810–3822.

[5] T. Mouton, X. Mercier, M. Wartel, N. Lamoureux, P. Desgroux, Laser-induced incandescence technique to identify soot nucleation and very small particles in low-pressure methane flames, Appl. Phys. B. 112 (2013) 369–379.

[6] J. Simonsson, N.-E. Olofsson, S. Török, P.-E. Bengtsson, H. Bladh, Wavelength dependence of extinction in sooting flat premixed flames in the visible and near-infrared regimes, Appl. Phys. B. 119 (2015) 657–667.

[7] Y. Wang, S.H. Chung, Soot formation in laminar counterflow flames, Progress in Energy and Combustion Science. 74 (2019) 152–238.

[8] C. Leermakers, C. Luijten, L.M.T. Somers, G. Kalghatgi, B. Albrecht, Experimental Study of Fuel Composition Impact on PCCI Combustion in a Heavy-Duty Diesel Engine, SAE Technical Papers. 2011-01–1351 (2011).

[9] L.S. Tran, B. Sirjean, P.-A. Glaude, R. Fournet, F. Battin-Leclerc, Progress in detailed kinetic modeling of the combustion of oxygenated components of biofuels, Energy. 43 (2012) 4–18.

[10] M. Fenkl, M. Pechout, M. Vojtisek, N-butanol and isobutanol as alternatives to gasoline: Comparison of port fuel injector characteristics, EPJ Web of Conferences. 114 (2016) 02021.

[11] J. Elias, A. Faccinetto, S. Batut, O. Carrivain, M. Sirignano, A. D'Anna, X. Mercier, Thermocouple-based thermometry for laminar sooting flames: Implementation of a fast and simple methodology, Int. J. Therm. Sci. 184 (2023) 107973.

[12] H.A. Michelsen, C. Schulz, G.J. Smallwood, S. Will, Laser-induced incandescence: Particulate diagnostics for combustion, atmospheric, and industrial applications, Progress in Energy and Combustion Science. 51 (2015) 2–48. https://doi.org/10.1016/j.pecs.2015.07.001.

[13] J. Yon, R. Lemaire, E. Therssen, P. Desgroux, A. Coppalle, K.F. Ren, Examination of wavelength dependent soot optical properties of diesel and diesel/rapeseed methyl ester mixture by extinction spectra analysis and LII measurements, Appl. Phys. B. 104 (2011) 253–271.

[14] C. Betrancourt, X. Mercier, F. Liu, P. Desgroux, Quantitative measurement of volume fraction profiles of soot of different maturities in premixed flames by extinction-calibrated laser-induced incandescence, Appl. Phys. B. 125 (2019) 16.